

ARTICLE TYPE**Detection of a centrifugal magnetosphere in one of the most massive stars in the ρ Oph star-forming cloud**S. Hubrig*¹ | M. Schöller² | S. P. Järvinen¹ | M. Küker¹ | A. F. Kholtygin³ | P. Steinbrunner⁴¹Leibniz-Institut für Astrophysik Potsdam (AIP), An der Sternwarte 16, 14482 Potsdam, Germany²European Southern Observatory, Karl-Schwarzschild-Str. 2, 85748 Garching, Germany³Astronomical Institute, Saint-Petersburg State University, Universitetskij pr. 28, 198504 Saint-Petersburg, Russia⁴Freie Universität Berlin, Kaiserswerther Str. 16-18, 14195 Berlin, Germany**Correspondence**

*Svetlana Hubrig. Email: shubrig@aip.de

Recent XMM-Newton observations of the B2 type star ρ Oph A indicated a periodicity of 1.205 d, which was ascribed to rotational modulation. Since variability of X-ray emission in massive stars is frequently the signature of a magnetic field, we investigated whether the presence of a magnetic field can indeed be invoked to explain the observed X-ray peculiarity. Two FORS 2 spectropolarimetric observations in different rotation phases revealed the presence of a negative ($\langle B_z \rangle_{\text{all}} = -419 \pm 101$ G) and positive ($\langle B_z \rangle_{\text{all}} = 538 \pm 69$ G) longitudinal magnetic field, respectively. We estimate a lower limit for the dipole strength as $B_d = 1.9 \pm 0.2$ kG. Our calculations of the Kepler and Alfvén radii imply the presence of a centrifugally supported, magnetically confined plasma around ρ Oph A. The study of the spectral variability indicates a behaviour similar to that observed in typical magnetic early-type Bp stars.

KEYWORDS:stars: early-type, stars: individual: ρ Oph A, stars: magnetic field, stars: variables: general, stars: formation, stars: X-rays**1 | INTRODUCTION**

The ρ Ophiuchus star-forming cloud is one of the closest low to intermediate mass star-forming regions and is known to contain the star-forming cluster LDN 1688. Due to its youth, the relative proximity (120–160 pc; e.g. Motte et al., 1998), and its richness in young stars and protostars, the ρ Oph star-forming cloud has been actively investigated in recent years, using multiwavelength observations from X-ray to radio bands.

The radiation field in LDN 1688 is dominated by two B-type stars, ρ Oph A (HD 147933) and ρ Oph B (HD 147934), both of spectral type B2V (Abergel et al., 1996), making up the visual binary system ρ Oph AB. The apparent distance between the two stars is about $3''$, and their orbital period is around 2400 yr. ρ Oph AB is surrounded by the bright and extended blue reflection nebula vdB 105. The basic structure of the cloud complex and its surroundings is described in detail by Wilking et al. (2008).

Massive young stars are known to emit strong X-rays. Unlike the X-ray emission from lower mass stars, which arises in stellar photospheres, the X-rays from massive stars are thought to result from powerful shocks. Detection of hard X-ray emission in massive stars appears frequently to be a signature of the presence of strong magnetic fields (e.g. Skinner et al., 2008). The first XMM-Newton observations of ρ Oph AB over 53 ks were obtained by Pillitteri et al. (2014). Their analysis showed a smooth variability of the X-ray emission, probably caused by the emergence of an extended active region on the surface of ρ Oph A. The derived hardness ratios were periodic, with the hardest spectrum corresponding to the highest count rate. According to Pillitteri et al. (2014), the observations are fully compatible with the hypothesis of the presence of a region brighter and hotter than the average stellar surface that gradually appears on the visible side of the star during the rise of the count rate. Follow-up XMM-Newton observations with a duration of 140 ks in 2016 allowed Pillitteri et al. (2017) to detect a periodicity of 1.205 d, which they ascribed to rotational modulation of the X-ray emission. Analysing the time resolved X-ray spectra, the authors speculated that either intrinsic magnetism

produces a hot spot on the surface of ρ Oph A, or an unknown low mass companion is the source of the observed X-ray variability. Clearly, the remarkable behavior of ρ Oph A in X-rays deserves further investigations to find out whether the presence of a magnetic field can indeed be invoked to explain the observed X-ray peculiarity.

In Section 2, we give an overview about the FORS 2 spectropolarimetric observations of ρ Oph A as well as the data reduction, and describe the results of the magnetic field measurements. The magnetospheric parameters and our analysis of the spectral variability of ρ Oph A are shown in Sections 3 and 4. A discussion of our results is presented in Section 5.

2 | OBSERVATIONS AND MAGNETIC FIELD MEASUREMENTS

FOcal Reducer and low dispersion Spectrograph (FORS 2; Appenzeller et al., 1998) spectropolarimetric observations of ρ Oph A were obtained on 2017 July 17 and August 11. The FORS 2 multi-mode instrument is equipped with polarisation analysing optics comprising super-achromatic half-wave and quarter-wave phase retarder plates, and a Wollaston prism with a beam divergence of $22''$ in standard resolution mode. We used the GRISM 600B and the narrowest available slit width of 0.4 to obtain a spectral resolving power of $R \approx 2000$. The observed spectral range from 3250 to 6215 Å includes all Balmer lines, apart from $H\alpha$, and numerous helium lines. For the observations, we used a non-standard readout mode with low gain (200kHz, 1x1, low), which provides a broader dynamic range, hence allowed us to reach a higher signal-to-noise ratio (SNR) in the individual spectra.

A first description of the assessment of longitudinal magnetic field measurements using FORS 1/2 spectropolarimetric observations was presented in our previous work (e.g. Hubrig et al., 2004a, 2004b, and references therein). To minimize the cross-talk effect, and to cancel errors from different transmission properties of the two polarised beams, a sequence of subexposures at the retarder position angles $-45^\circ+45^\circ$, $+45^\circ-45^\circ$, $-45^\circ+45^\circ$, etc. is usually executed during the observations. Moreover, the reversal of the quarter wave plate compensates for errors in the relative wavelength calibrations of the two polarised spectra. According to the FORS User Manual, the V/I spectrum is calculated using:

$$\frac{V}{I} = \frac{1}{2} \left\{ \left(\frac{f^o - f^e}{f^o + f^e} \right)_{-45^\circ} - \left(\frac{f^o - f^e}{f^o + f^e} \right)_{+45^\circ} \right\}, \quad (1)$$

where $+45^\circ$ and -45° indicate the position angle of the retarder waveplate and f^o and f^e are the ordinary and the extraordinary beam, respectively. Null profiles, N , are calculated as pairwise differences from all available V profiles.

From these, 3σ -outliers are identified and used to clip the V profiles. This removes spurious signals, which mostly come from cosmic rays, and also reduces the noise. A full description of the updated data reduction and analysis will be presented in a separate paper (Schöller et al., in preparation, see also Hubrig et al., 2014a). The mean longitudinal magnetic field, $\langle B_z \rangle$, is measured on the rectified and clipped spectra based on the relation following the method suggested by Angel & Landstreet (1970)

$$\frac{V}{I} = -\frac{g_{\text{eff}} e \lambda^2}{4\pi m_e c^2} \frac{1}{I} \frac{dI}{d\lambda} \langle B_z \rangle, \quad (2)$$

where V is the Stokes parameter that measures the circular polarization, I is the intensity in the unpolarized spectrum, g_{eff} is the effective Landé factor, e is the electron charge, λ is the wavelength, m_e is the electron mass, c is the speed of light, $dI/d\lambda$ is the wavelength derivative of Stokes I , and $\langle B_z \rangle$ is the mean longitudinal (line-of-sight) magnetic field.

The longitudinal magnetic field was measured in two ways: using the entire spectrum including all available lines or using exclusively the hydrogen lines. Furthermore, we have carried out Monte Carlo bootstrapping tests. These are most often applied with the purpose of deriving robust estimates of standard errors. The measurement uncertainties obtained before and after the Monte Carlo bootstrapping tests were found to be in close agreement, indicating the absence of reduction flaws. The results of our magnetic field measurements, those for the entire spectrum or only for the hydrogen lines, are presented in Table 1. As no ephemeris is known for ρ Oph A – only $P_{\text{rot}} = 1.205$ d is mentioned in Pillitteri et al. (2017) – we fixed the rotation phase 0 at the date of the first FORS 2 observation at MJD 57951.2242.

The magnetic field of ρ Oph A was detected on both observing dates. Using the entire spectrum, we measure a field of negative polarity, $\langle B_z \rangle_{\text{all}} = -419 \pm 101$ G, at a significance level of 4.1σ in the data obtained on 2017 July 17, while the measurement using the hydrogen lines shows a significance of 2.1σ . The highest values for the longitudinal magnetic field, $\langle B_z \rangle_{\text{all}} = 538 \pm 69$ G at a significance level of 7.8σ using the entire spectrum and $\langle B_z \rangle_{\text{hyd}} = 569 \pm 94$ G at a significance level of 6.1σ using the hydrogen lines was measured in the data obtained on 2017 August 11. No detection was achieved in the diagnostic N spectra, indicating the absence of spurious polarization signatures.

In Figs. 1 and 2, we show the linear regressions in plots of V/I against $-4.67 \cdot 10^{-13} \lambda^2 (1/I)(dI/d\lambda)$ together with the results of the Monte Carlo bootstrapping tests. In Fig. 3, we present Stokes I , V , and diagnostic N spectra of ρ Oph A obtained on 2017 August 11 in the spectral region around the $H\beta$ line and several He I lines.

TABLE 1 Logbook of the FORS 2 spectropolarimetric observations of ρ Oph A, including the modified Julian date of mid-exposure, followed by the achieved signal-to-noise ratio in the Stokes I spectra around 5200 Å, and the measurements of the mean longitudinal magnetic field using the Monte Carlo bootstrapping test, for all lines and for the hydrogen lines. In the last columns, we present the results of our measurements using the null spectra for the set of all lines and the orbital phases. The rotation phases of ρ Oph A are calculated relative to a zero phase corresponding to the date of the first FORS 2 observation at MJD 57951.2242 assuming $P_{\text{rot}} = 1.205$ d. All quoted errors are 1σ uncertainties.

MJD	SNR $\lambda 5200$	$\langle B_z \rangle_{\text{all}}$ [G]	$\langle B_z \rangle_{\text{hyd}}$ [G]	$\langle B_z \rangle_{\text{N}}$ [G]	φ_{orb}
57951.2242	2297	-419 ± 101	-301 ± 142	-72 ± 92	0
57976.0708	3005	538 ± 69	569 ± 94	29 ± 68	0.620

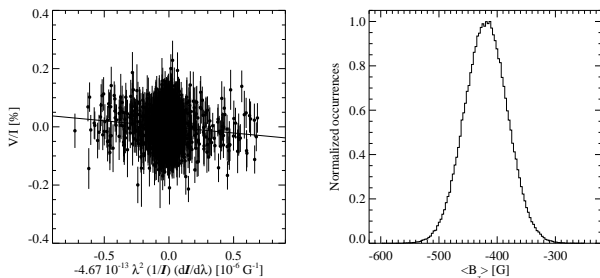


FIGURE 1 *Left panel:* Linear fit to Stokes V obtained for the FORS 2 observation of ρ Oph A on MJD 57951.2242. *Right panel:* Distribution of the longitudinal magnetic field values $P(\langle B_z \rangle)$, which were obtained via bootstrapping. From this distribution follows the most likely value for the longitudinal magnetic field $\langle B_z \rangle_{\text{all}} = -419 \pm 101$ G.

We can estimate the dipole strength of ρ Oph A following the model by Stibbs (1950) as formulated by Preston (1967):

$$B_d \geq \langle B_z \rangle^{\max} \left(\frac{15+u}{20(3-u)} \right)^{-1}. \quad (3)$$

Assuming a limb-darkening coefficient u of 0.3, typical for the spectral type B2V (Claret & Bloemen, 2011), we can give a lower limit for the dipole strength of $B_d \geq 1.9 \pm 0.2$ kG.

3 | MAGNETOSPHERIC PARAMETERS

Similar to the small number of previously studied early-B type stars, the X-ray emission in ρ Oph A detected in XMM-Newton observations can be generated via magnetically confined shocks. Babel & Montmerle (1997) suggested that in stars with large-scale magnetic fields wind streams from opposite hemispheres are channeled toward the magnetic equator, where they collide, leading to strong shocks and associated X-rays. To investigate whether the wind plasma is locked to the magnetic field, we need to know several physical parameters

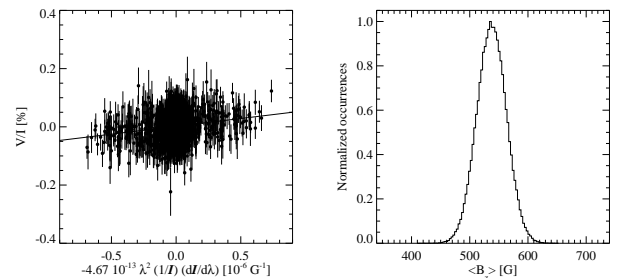


FIGURE 2 *Left panel:* Linear fit to Stokes V obtained for the FORS 2 observation of ρ Oph A on MJD 57976.0708. *Right panel:* Distribution of the longitudinal magnetic field values $P(\langle B_z \rangle)$, which were obtained via bootstrapping. From this distribution follows the most likely value for the longitudinal magnetic field $\langle B_z \rangle_{\text{all}} = 538 \pm 69$ G.

of ρ Oph A. Currently, the only information can be found in the work of Pillitteri et al. (2017), who assumed a stellar radius of $\sim 8 R_{\odot}$, without mentioning the method of estimation, used the rotational modulation of the X-ray emission to determine a rotation period of 1.205 d, and applied a Fourier transform to the He I 6678 line to measure $v \sin i = 239.5 \pm 10$ km s $^{-1}$.

Based on revised trigonometric parallaxes from the Hipparcos data (van Leeuwen, 2008), Mamajek (2008) concluded that a distance of 131 ± 3 pc to the Ophiuchus star-forming region is the best available derived from Hipparcos data. Using this distance, the extinction $A_v = 3$ from Pillitteri et al. (2016), assuming $T_{\text{eff}} = 21000$ K for the spectral type B2 (Böhm-Vitense, 1981), and the corresponding bolometric correction $BC = -2.0 \pm 0.1$ (Flower, 1996), we estimate $\log(L/L_{\odot}) = 4.1 \pm 0.2$, taking into account estimation inaccuracies of the distance determination and the bolometric correction. From the position of ρ Oph A in the H-R diagram, using evolutionary tracks from Ekström et al. (2012) and assuming that ρ Oph A is still in the hydrogen fusing stage, we find a mass of about $10 \pm 0.7 M_{\odot}$. From the Stefan-Boltzmann law we find $\log(R/R_{\odot}) \approx 0.93$, i.e. a value of

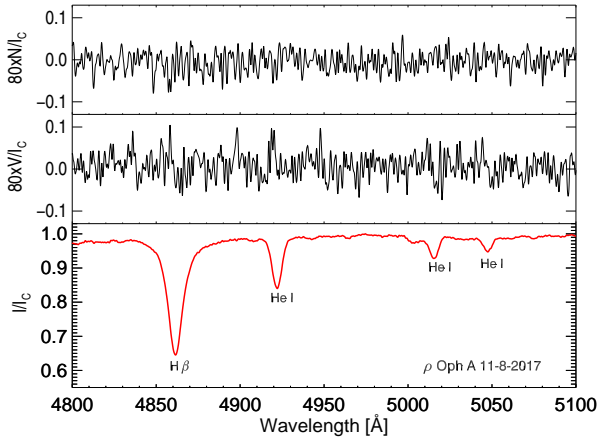


FIGURE 3 Stokes I , V , and diagnostic N spectra (from bottom to top) of ρ Oph A in the vicinity of the $H\beta$ line. Note that the Stokes V and the diagnostic N spectra were magnified by a factor of 80.

$8.5 \pm 1 R_{\odot}$ for the stellar radius. Using this radius, $v \sin i = 240 \pm 10 \text{ km s}^{-1}$, and the rotation period $P_{\text{rot}} = 1.205 \text{ d}$, we obtain $v_{\text{eq}} = 360 \pm 40 \text{ km s}^{-1}$ and an inclination angle of the stellar rotation axis to the line of sight $i = 42 \pm 6^{\circ}$. Further, the rotation period of 1.205 d corresponds to an angular velocity $\Omega = 6.035 \times 10^{-5} \text{ s}^{-1}$. To determine the properties of the stellar wind and the magnetosphere, we first compute the escape velocity, $v_{\text{esc}} = \sqrt{2GM/R} = 671 \text{ km s}^{-1}$. Assuming that $v_{\infty}/v_{\text{esc}} = 1.3$ (Vink et al., 2001), we find $v_{\infty} = 873 \text{ km s}^{-1}$ for the terminal velocity. Using equation (25) of Vink et al. (2001), we calculate a mass loss rate $\dot{M} = 8.69 \times 10^{-9} M_{\odot}/\text{yr}$ for solar metallicity. With a polar magnetic field strength $B_p \geq 1.9 \text{ kG}$, we obtain a confinement parameter $\eta_* = (B_{\text{eq}}^2 R_*^2)/(\dot{M} v_{\infty}) \geq 6.55 \times 10^4$, where $B_{\text{eq}} = 0.5 B_p$ (ud-Doula & Owocki, 2002). The impact of rotation is measured by the parameter $W = \Omega R/v_K = 0.75$, where $v_K = \sqrt{GM/R}$. Using equation (9) from ud-Doula et al. (2008), we thus arrive at $R_A = (0.3 + (\eta_* + 0.25)^{1/4}) R_* \geq 9.3 R_*$ for the Alfvén radius and $R_K = (GM/\Omega^2)^{1/3} = 1.21 R_*$ for the Kepler (corotation) radius.

Petit et al. (2013) divided magnetic massive stars into two groups, those with dynamical magnetospheres (DMs) with $R_A < R_K$ and those possessing centrifugal magnetospheres (CMs) with $R_A > R_K$. Since for ρ Oph A the radial extent of the magnetic confinement of the wind given by the Alfvén radius is much larger than the Kepler radius, material caught in the region between R_A and R_K is centrifugally supported against infall, and so builds up to a much denser CM.

The rotational modulation of the X-ray emission with $P_{\text{rot}} = 1.205 \text{ d}$ detected by Pillitteri et al. (2017) possibly indicates that the wind plasma is predominantly locked to the magnetic

field and that the magnetosphere of ρ Oph A can be interpreted in the context of the rigidly rotating magnetosphere model (RRM; Townsend & Owocki, 2005). A few rapidly rotating early-B type stars with RRM magnetospheres showing comparable rotation periods and magnetic field strengths were discovered in the last years (e.g., Rivinius et al., 2013, Eikenberry et al., 2014). As is shown in Fig. 4, the spectral appearance of ρ Oph A in our FORS 2 observations is very similar to the spectral appearance of two other rapidly rotating early-B type stars, HD 23478 ($P_{\text{rot}} = 1.05 \text{ d}$) and HD 345439 ($P_{\text{rot}} = 0.77 \text{ d}$), for which the presence of RRM was recently detected (Eikenberry et al., 2014). In all stars with RRM, the cooler and denser postshock material trapped in the stellar magnetospheres is typically detected in the $H\alpha$ line or in the near infrared hydrogen recombination lines. Since our FORS 2 polarimetric spectra of ρ Oph A do not cover the spectral region containing the $H\alpha$ line, it would be valuable to monitor the variability of the $H\alpha$ line profile in future observations to confirm that circumstellar gas is locked to the magnetosphere and is in corotation with the stellar surface.

4 | SPECTRAL VARIABILITY

In early-B type magnetic Bp stars, the global magnetic dipole-like field is tilted to the rotation axis by the angle β and the surface distribution of certain chemical elements, such as silicon or carbon, displays a spotted structure, which is, as a rule, disjunct from the helium distribution. As the star rotates, we should detect variations in the strength of the longitudinal magnetic field and the intensities of spectral line profiles of various elements with the rotation period of the star. Since our observations correspond to two different rotational phases, where opposite magnetic field polarities are detected, we have compared the line profile shapes on these two different epochs. Due to the rather low FORS 2 spectral resolution, we checked the variability only for hydrogen, helium, and silicon lines. Our comparison of the line profiles belonging to these elements presented in Fig. 5 reveals distinct changes in the line intensities of the helium lines, supporting the assumption of the presence of an inhomogeneous helium distribution on the stellar surface. We also detect that the $H\beta$ line intensity is lower in the phase where the helium line intensities are stronger. On the other hand, silicon lines are very weak and noisy and do not present any obvious variability. To check variability on a time scale of a few minutes, we compared the stability of the line profiles belonging to these elements over the full sequences of sub-exposures obtained on that time-scale. No short-term variability was detected in both FORS 2 observations.

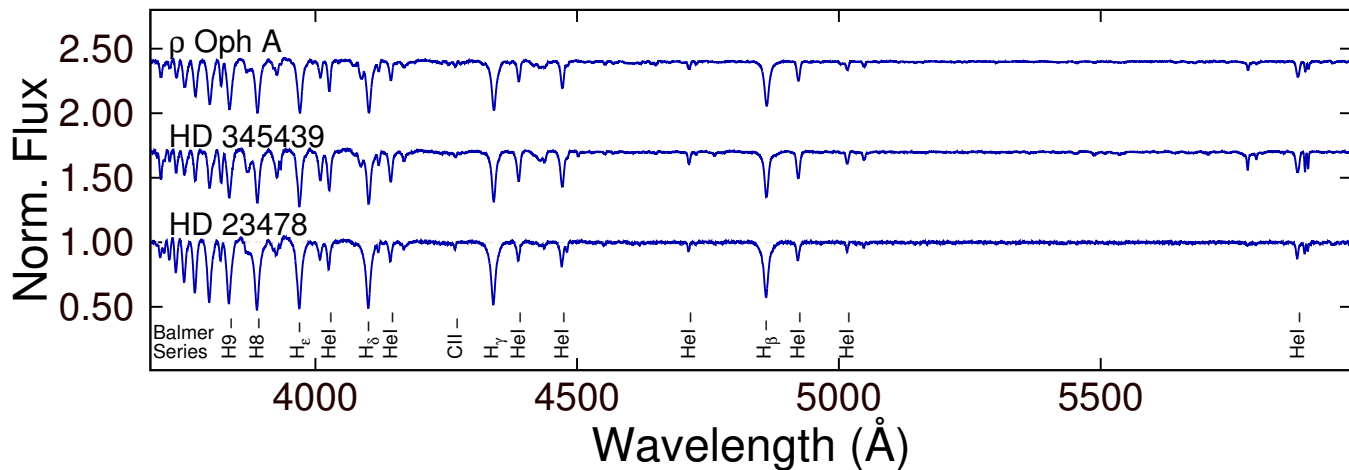


FIGURE 4 The normalized FORS 2 Stokes I spectrum of ρ Oph A is displayed together with the normalized FORS 2 spectra of two other rapidly rotating early-B type stars, HD 23478 and HD 345439, for which the presence of a rigidly rotating magnetosphere was recently detected (Eikenberry et al., 2014). Well known spectral lines are indicated. The spectra of HD 345439 and ρ Oph A were vertically offset for clarity.

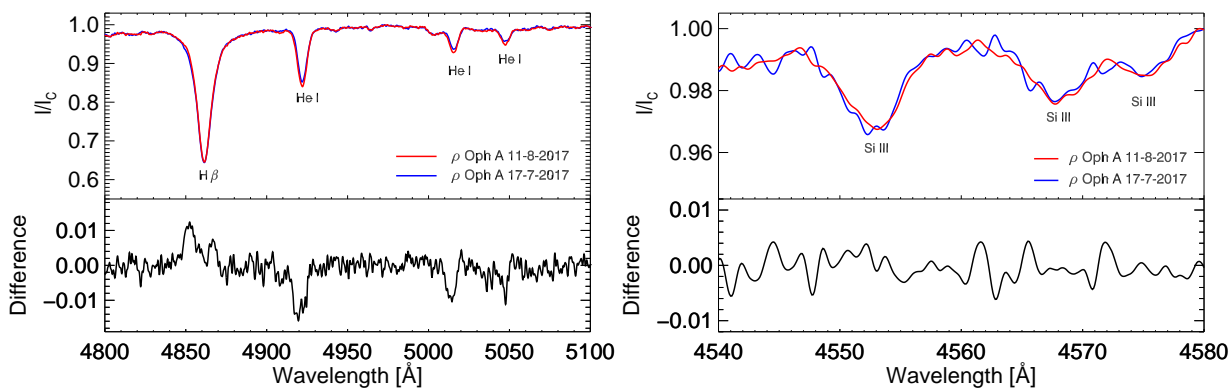


FIGURE 5 *Left panel:* Variability of the $H\beta$ and He I lines in the spectra of ρ Oph A. On the top one can see the normalized FORS 2 spectra obtained on two different nights. On the bottom, the difference between the two spectra is shown. *Right panel:* No variability is detected for the Si III lines at wavelengths 4553, 4567, and 4574 Å.

5 | DISCUSSION

The analysis of FORS 2 spectropolarimetric observations of ρ Oph A on two different rotation phases reveals the presence of a rather strong magnetic field with a dipole strength of $B_d \geq 1.9 \pm 0.2$ kG. Using physical parameters of this B2 type star, we calculated Kepler and Alfvén radii and concluded that a centrifugally supported, magnetically confined plasma is present around ρ Oph A. Since the magnetic field of ρ Oph A was measured only on two occasions, it should be a prime candidate for a follow-up spectropolarimetric study that would lead to more accurate magnetospheric parameters.

A comparison of line profiles on two different rotation phases shows a clear variability of helium lines similar to that

observed in typical magnetic early-type Bp stars. The variability of the $H\beta$ line can probably be explained by the presence of an extended magnetosphere around ρ Oph A. Based on our detection of the presence of a magnetic field in ρ Oph A, we conclude that the most likely reason for the variations of the X-ray emission observed by Pillitteri et al. (2017) is the occultation of parts of the magnetosphere by the stellar body.

The origin of magnetic fields in massive stars is still a major unresolved problem in astrophysics. Only a small fraction of stars (5–7%, e.g. Schöller et al., 2017) with radiative envelopes possess strong large-scale organized magnetic fields. Such fields can probably be generated during the star formation process, by dynamo action taking place in the rotating stellar cores, or they could be products of a merger process. While

the first two scenarios are unable to explain a number of observational phenomena (e.g. Ferrario et al., 2015), the magnetic fields might form when two protostellar objects merge late during their evolution towards the main sequence and when at least one of them has already acquired a radiative envelope (Ferrario et al., 2009).

ρ Oph A is not the only magnetic star detected in a complex star forming region. In 2013, using the High Accuracy Radial velocity Planet Searcher polarimeter (HARPSpol; Snik et al., 2008) attached to ESO's 3.6 m telescope (La Silla, Chile) and FORS 2 observations, Hubrig et al. (2014b) searched for the presence of a magnetic field in the three most massive central stars in the Trifid nebula, HD 164492A, HD 164492C, and HD 164492D. These observations indicated the presence of a strong longitudinal magnetic field of about 500–600 G in the poorly studied component HD 164492C. Later, González et al. (2017) showed that HD 164492C is a spectroscopic triple system consisting of an eccentric close spectroscopic binary with a period of 12.5 d, and a massive fast rotating He-rich tertiary possessing a variable kG order magnetic field. Similar to ρ Oph A, also in HD 164492C the X-ray emission was firmly detected using Chandra observations (Rho et al., 2004). The detection of magnetic massive stars in the youngest star-forming regions implies that these targets may play a pivotal role in our understanding of the origin of magnetic fields in massive stars. It is striking that both magnetic massive stars located in young star-forming regions show similar characteristics such as fast rotation and the presence of X-ray emission. Also their stellar surfaces show helium abundance variations typical for He-rich Bp stars with large-scale organized magnetic fields. Especially intriguing is the presence of an extended blue reflection nebula around the system ρ Oph AB: A few years ago, Hubrig (2013a) discussed the variability of the longitudinal magnetic field in the O6.5f?p star HD 148937 (Hubrig et al., 2008, 2013b), suggesting that this target may provide a smoking gun, as it is surrounded by the 3000 yr old, nitrogen-rich bipolar nebula NGC 6164/5 (Leitherer & Chavarria-K., 1987), which was likely created through strong binary interaction. In parallel with HD 148937, we can speculate that ρ Oph A can similarly be a merger product and that the surrounding nebula is created by the ejected material. Obviously, it would be important to investigate the chemical composition of the material of the nebula around ρ Oph A to determine its origin. Furthermore, since star formation in molecular clouds is assumed to be triggered by the dynamical action of winds from massive stars, we need to understand how magnetized winds from magnetic massive stars formed during the first episodes of star formation influence their environments, including nearby sites of star formation and protoplanetary disks surrounding low-mass pre-main-sequence stars.

ACKNOWLEDGMENTS

Based on observations made with ESO Telescopes at the La Silla Paranal Observatory under programme 099.D-0067(A). AK acknowledges financial support from RFBR grant 16-02-00604A.

REFERENCES

- Abergel, A., Bernard, J. P., Boulanger, F., et al. 1996, *A&A*, 315, L329
 Angel, J. R. P., Landstreet, J. D. 1970, *ApJ*, 160, L147
 Appenzeller, I., Fricke, K., Fürtig, W., et al. 1998, *The ESO Messenger*, 94, 1
 Babel, J., Montmerle, T. 1997, *A&A*, 323, 121
 Böhm-Vitense, E. 1981, *Ann. Rev. Astron. Astrophys.*, 19, 295
 Claret, A., Bloemen, S. 2011, *A&A*, 529, A75
 Eikenberry, S. S., Chojnowski, S. D., Wisniewski, J., et al. 2014, *ApJL*, 784, L30
 Ekström, S., Georgy, C., Eggenberger, P., et al. 2012, *A&A*, 537, A146
 Ferrario, L., Pringle, J. E., Tout, C. A., Wickramasinghe, D. T. 2009, *MNRAS*, 400, L71
 Ferrario, L., Melatos, A., Zrake, J. 2015, *Space Sci. Rev.*, 191, 77
 Flower, P. J. 1996, *ApJ*, 469, 355
 González, J. F., Hubrig, S., Przybilla, N., et al. 2017, *MNRAS*, 467, 437
 Howarth, I. D., Stevens, I. R. 2014, *MNRAS*, 445, 2878
 Hubrig, S., Kurtz, D. W., Bagnulo, S., et al. 2004a, *A&A*, 415, 661
 Hubrig, S., Szeifert, T., Schöller, M., et al. 2004b, *A&A*, 415, 685
 Hubrig, S., Schöller, M., Schnerr, R. S., et al. 2008, *A&A*, 490, 793
 Hubrig, S. 2013a, in: "Massive Stars: From α to Ω ", held 10–14 June 2013 in Rhodes, Greece; online at <http://a2omega-conference.net>, id. 39
 Hubrig, S., Schöller, M., Ilyin, I., et al. 2013b, *A&A*, 551, A33
 Hubrig, S., Schöller, M., Kholtygin, A. F. 2014a, *MNRAS*, 440, 1779
 Hubrig, S., Fossati, L., Carroll, T. A., et al. 2014b, *A&A*, 564, L1
 Leitherer, C., Chavarria-K., C. 1987, *A&A*, 175, 208
 Maheswaran, M., Cassinelli, J. P. 2009, *MNRAS*, 394, 415
 Mamajek, E. E. 2008, *AN*, 329, 10
 Motte, F., Andre, P., Neri, R. 1998, *A&A*, 336, 150
 Petit, V., Owocki, S. P., Wade, G. A., et al. 2013, *MNRAS*, 429, 398
 Pillitteri, I., Wolk, S. J., Goodman, A., Sciortino, S. 2014, *A&A*, 567, L4
 Pillitteri, I., Wolk, S. J., Chen, H. H., Goodman, A. 2016, *A&A*, 592, A88
 Pillitteri, I., Wolk, S. J., Reale, F., Oskinova, L. 2017, *A&A*, 602, A92
 Preston, G. W. 1967, *ApJ*, 150, 547
 Rho, J., Corcoran, M. F., Hamaguchi, K., Lefloch, B. 2004, *ApJ*, 607, 904
 Rivinius, T., Townsend, R. H. D., Kochukhov, O., et al. 2013, *MNRAS*, 429, 177
 Schöller, M., Hubrig, S., Fossati, L., et al. 2017, *A&A*, 599, A66
 Skinner, S. L., Sokal, K. R., Cohen, D. H., et al. 2008, *ApJ*, 683, 796
 Snik, F., Jeffers, S., Keller, Ch., et al. 2008, *Proc. SPIE*, 7014, E22
 Stibbs, D. W. N. 1950, *MNRAS*, 110, 395
 Townsend, R. H. D., Owocki, S. P. 2005, *MNRAS*, 357, 251
 ud-Doula, A., Owocki, S. P. 2002, *ApJ*, 576, 413
 ud-Doula, A., Owocki, S. P., Townsend, R. H. D. 2008, *MNRAS*, 385, 97
 van Leeuwen, F. 2008, *VizieR Online Data Catalog: Hipparcos, the New Reduction, Cat. 1311*

Vink, J. S., de Koter, A., Lamers, H. J. G. L. M. 2001, A&A, 369, 574
Wilking, B. A., Gagné, M., Allen, L. E. 2008, "Handbook of Star
Forming Regions, Volume II: The Southern Sky", ASP Mono-
graph Publications, Vol. 5. Edited by Bo Reipurth, p. 351

